Journal of Geophysical Research: Space Physics

Supporting Information for

Juno's multi-instruments observations during the flybys of auroral bright spots in Jupiter's polar aurorae

K. Haewsantati[1,2,3], B. Bonfond[1], S. Wannawichian[3,4], G. R. Gladstone[5], V. Hue[5,6], T. K. Greathouse[5], D. Grodent[1], Z. Yao[7,1], J.-C. Gérard[1], R. Guo[8,1], S. Elliott[9,10], B. H. Mauk[11], G. Clark[11], D. Gershman[12], S. Kotsiaros[13], W. S. Kurth[9], J. Connerney[12], J. R. Szalay[14], A. Phriksee[3]

[1]LPAP, STAR Institute, Université de Liège, Liège, Belgium
[2]Ph.D. program in Physics, Department of Physics and Materials Science, Faculty of Science, Chiang Mai University, Chiang Mai, Thailand
[3]National Astronomical Research Institute of Thailand (Public Organization), Chiang Mai, Thailand [4]Department of Physics and Materials Science, Faculty of Science, Chiang Mai University, Chiang Mai, Thailand
[5]Southwest Research Institute, San Antonio, Texas, USA
[6]Aix-Marseille Université, CNRS, CNES, Institut Origines, LAM, Marseille, France
[7]Key Laboratory of Earth and Planetary Physics, Institute of Geology and Geophysics, Chinese Academy of Sciences, Beijing, China
[8]Laboratory of Optical Astronomy and Solar-Terrestrial Environment, Institute of Space Sciences, School of Space Science and Physics, Shandong University, Weihai, Shandong, China
[9]Department of Physics and Astronomy, University of Iowa, Iowa City, IA, USA
[10]School of Physics and Astronomy, University of Minnesota, Minneapolis, MN, USA
[11]The Johns Hopkins University Applied Physics Laboratory, Laurel, MD, USA
[12]NASA Goddard Space Flight Center, Greenbelt, MD, USA
[13]DTU Space, Technical University of Denmark (DTU), Kongens Lyngby, Denmark
[14]Department of Astrophysical Sciences, Princeton University, Princeton, NJ, USA

Contents of this file

Introduction

The additional information provided here are:

1. The observed magnetic field in each component with the data from JRM33(order 18) + Con2020 and the 5th-degree polynomial fit. The codes to calculate the JRM33 (order 18) model of Jupiter's internal magnetic field model (Connerney et al., 2022) and the magnetodisc model (Connerney et al., 2020) are available at https://github.com/rjwilson-LASP/PSH and https://github.com/marissav06/con2020, respectively.

2. The electric field spectral density in details. We also over-plotted the electron and proton cyclotron frequencies to focus on the intensifications between these two characteristic frequencies. The E/cB ratio plots are provided to categorize the wave types.

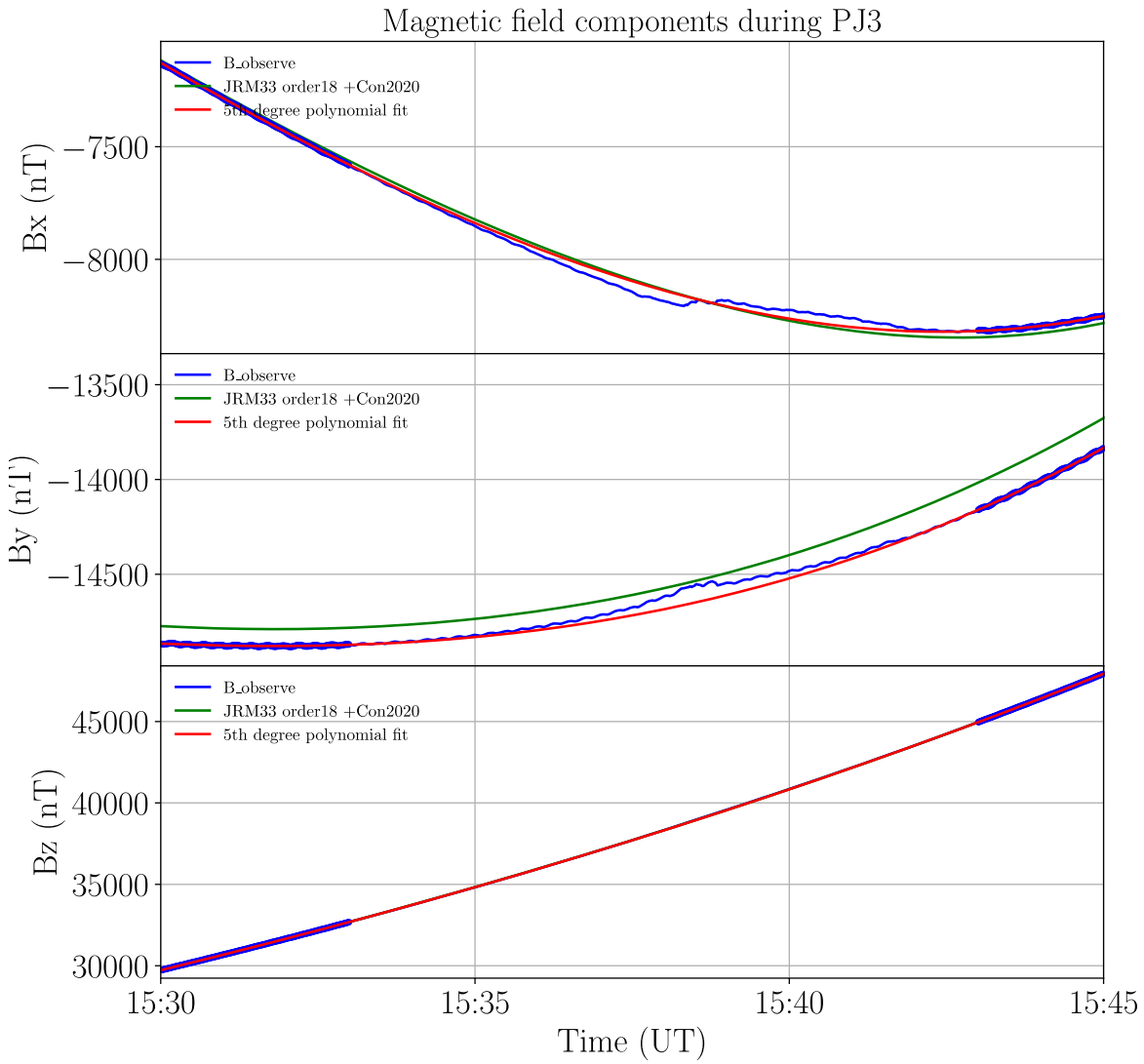

Figure S1. Three magnetic field components observed during PJ3 are obtained from MAG (blue lines), the JRM33(order 18) + Con2020 magnetic field model (green lines), and the 5th-degree polynomial fit (red lines) using observed data during the time intervals before (15:30-15:33) and after (15:43-15:45) bright spot crossing where magnetic perturbation (shaded region) could take place.

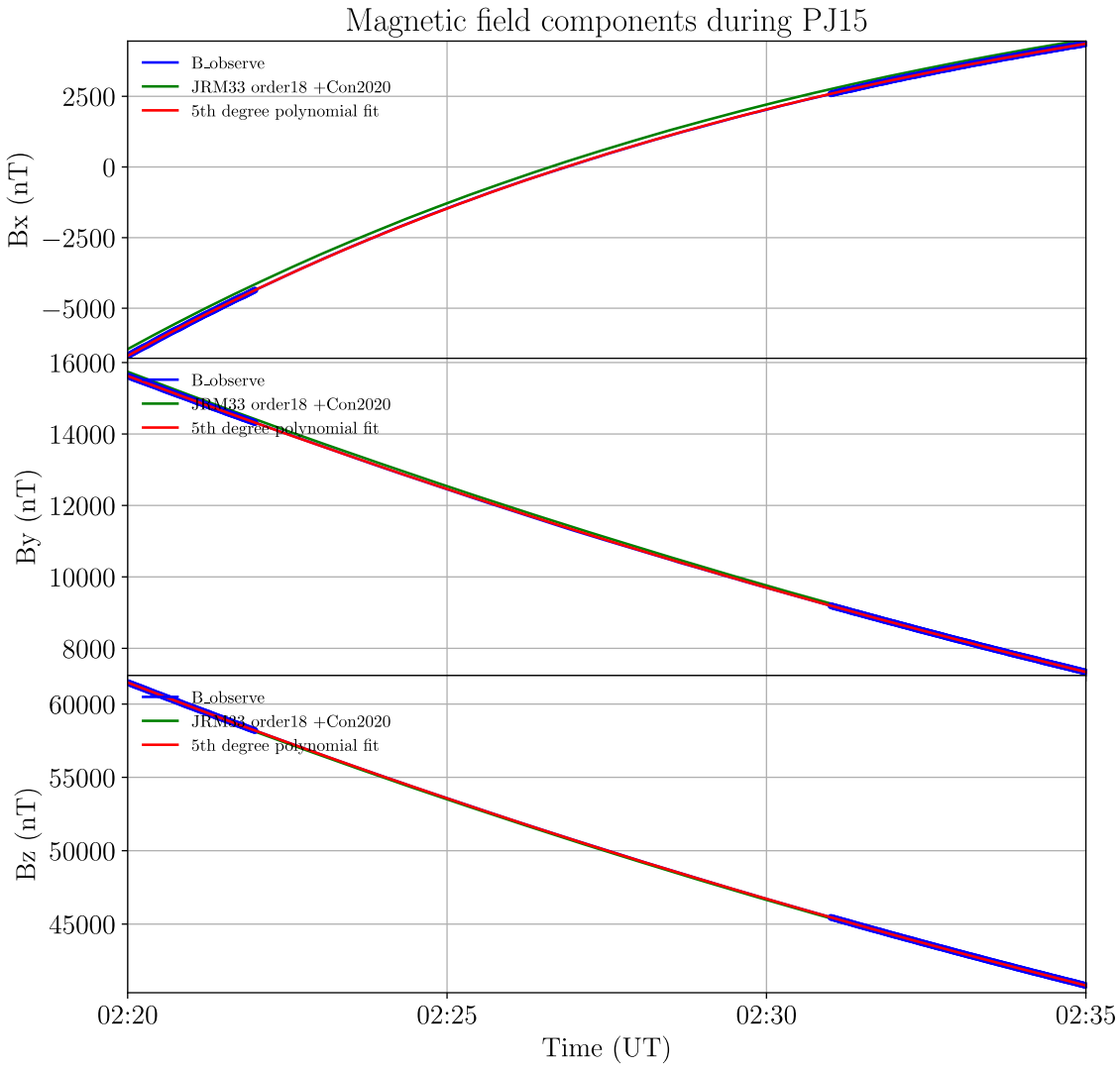

Figure S2. Three magnetic field components observed during PJ3 are obtained from MAG (blue lines), the JRM33(order 18) + Con2020 magnetic field model (green lines), and the 5th-degree polynomial fit (red lines) using observed data during the time intervals before (02:20-02:22) and after (02:31-02:35) bright spot crossing where magnetic perturbation (shaded region) could take place.

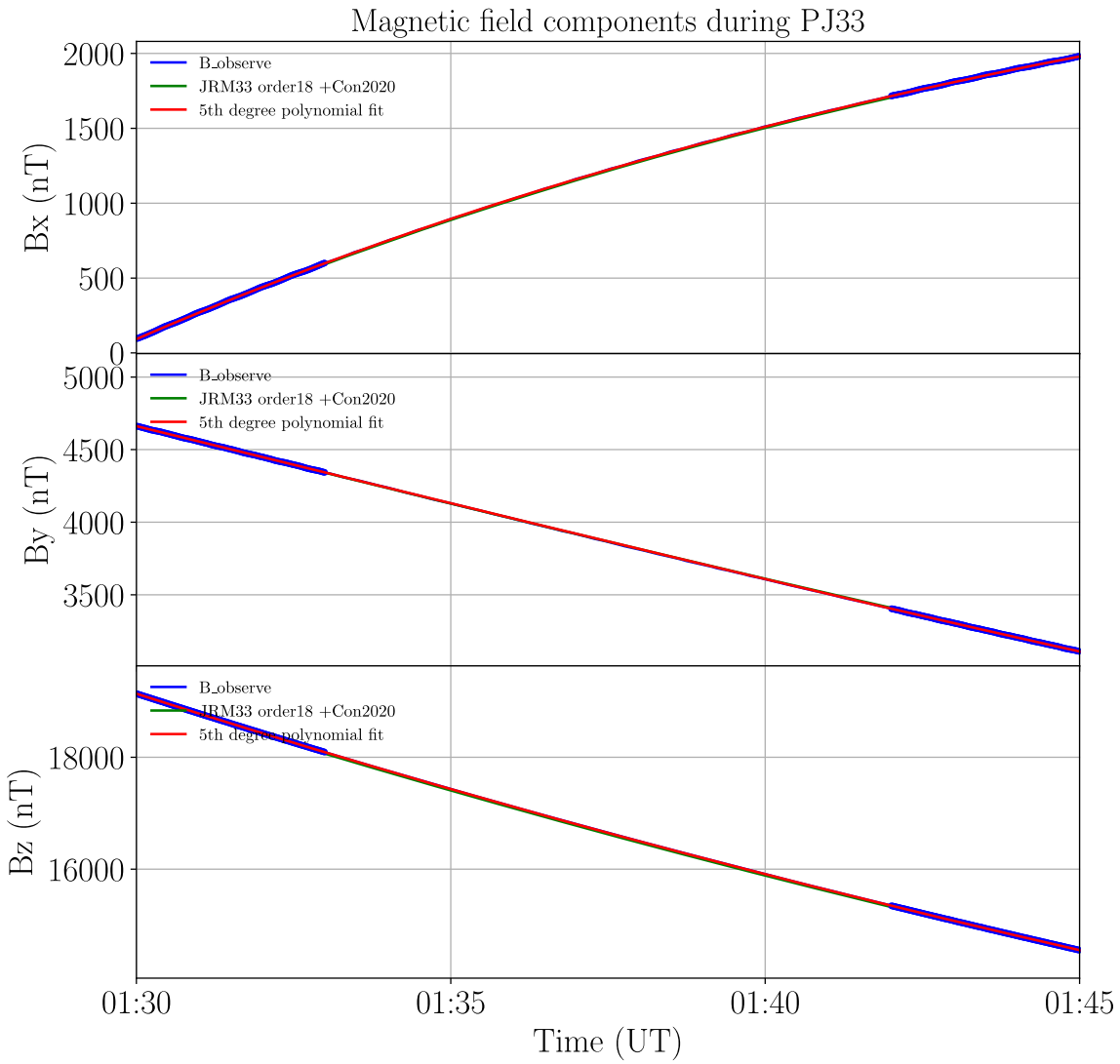

Figure S3. Three magnetic field components observed during PJ3 are obtained from MAG (blue lines), the JRM33(order 18) + Con2020 magnetic field model (green lines), and the 5th-degree polynomial fit (red lines) using observed data during the time intervals before (01:30-01:33) and after (01:43-01:45) bright spot crossing where magnetic perturbation (shaded region) could take place.

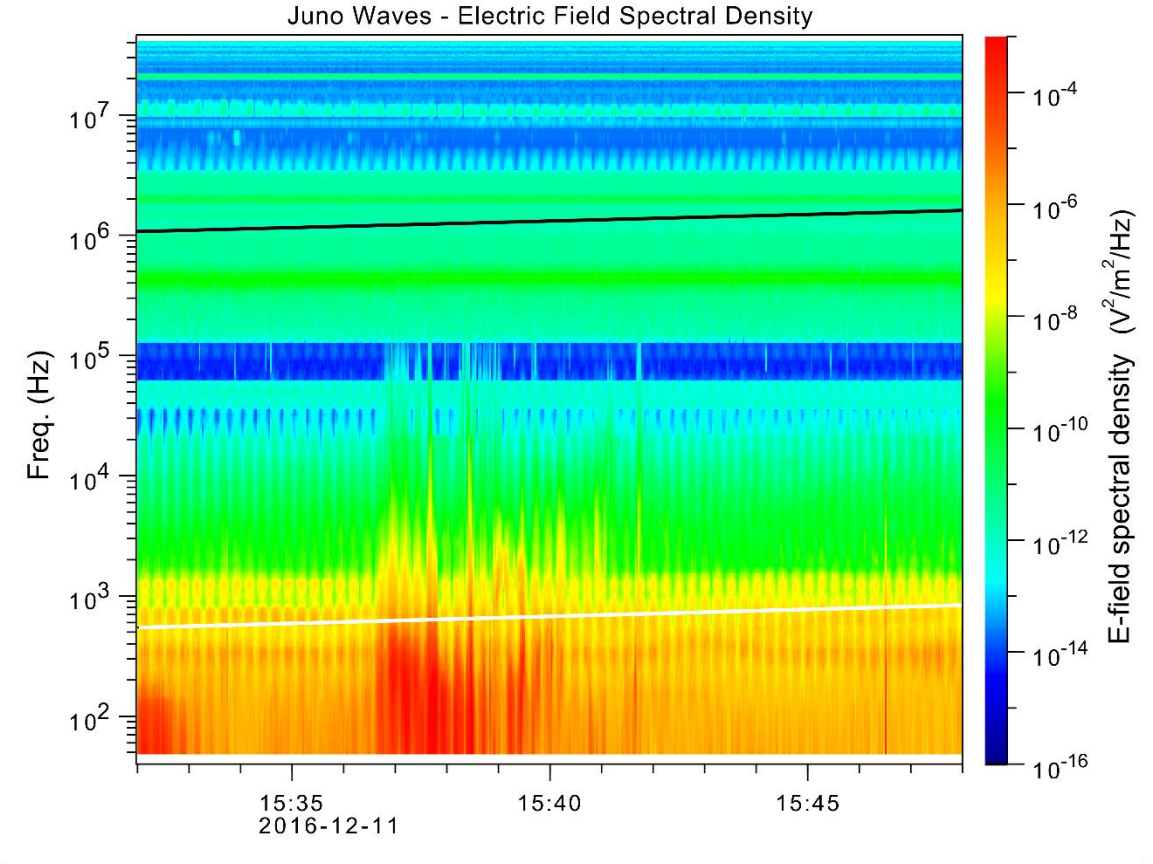

Figure S4. Electric field spectral density from whistler mode wave observations taken by Juno Waves instrument over the Jovian polar regions during PJ3. The black line indicates the range of electron cyclotron frequency, and the white line indicates the range of the proton cyclotron frequency.

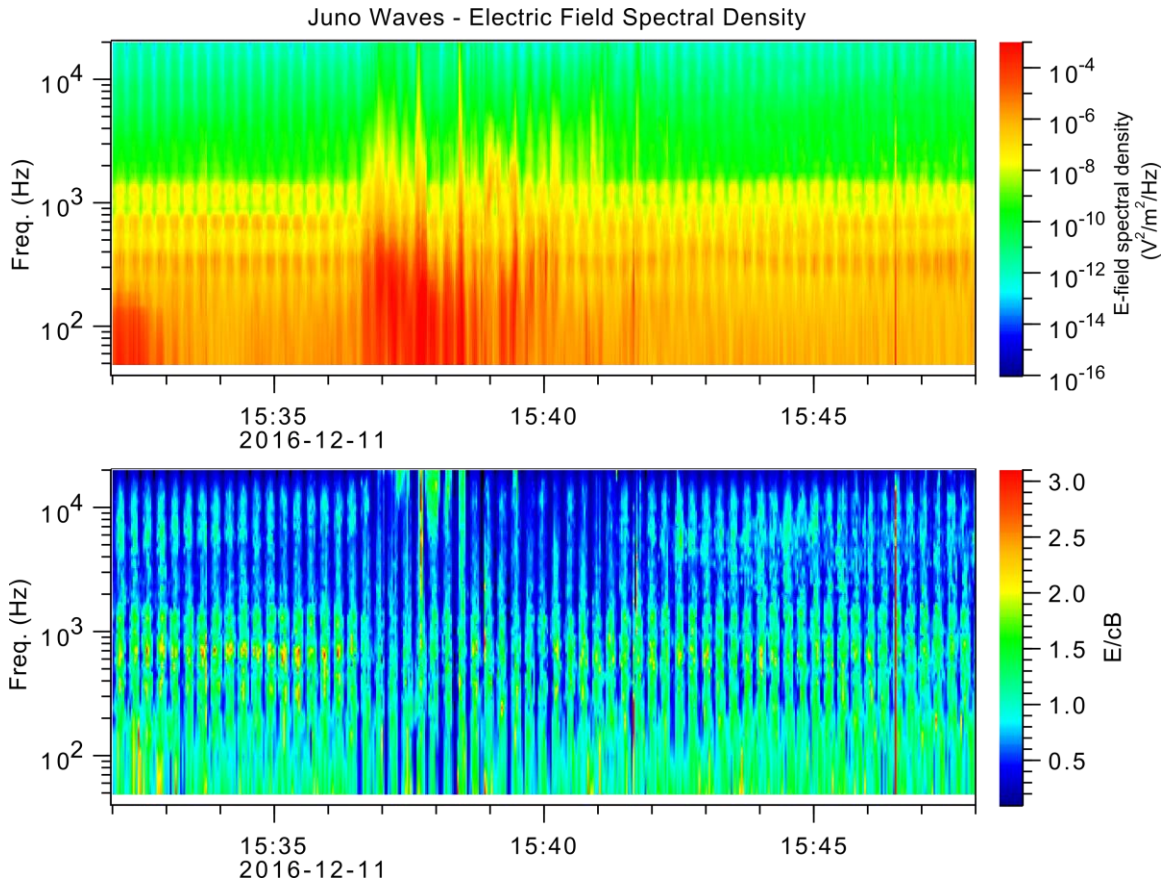

Figure S5. (Top) Electric field spectral density from whistler mode wave observations taken by Juno Waves instrument over the Jovian polar regions during PJ3. (Bottom) Frequency-time spectrogram of the E/cB ratio.

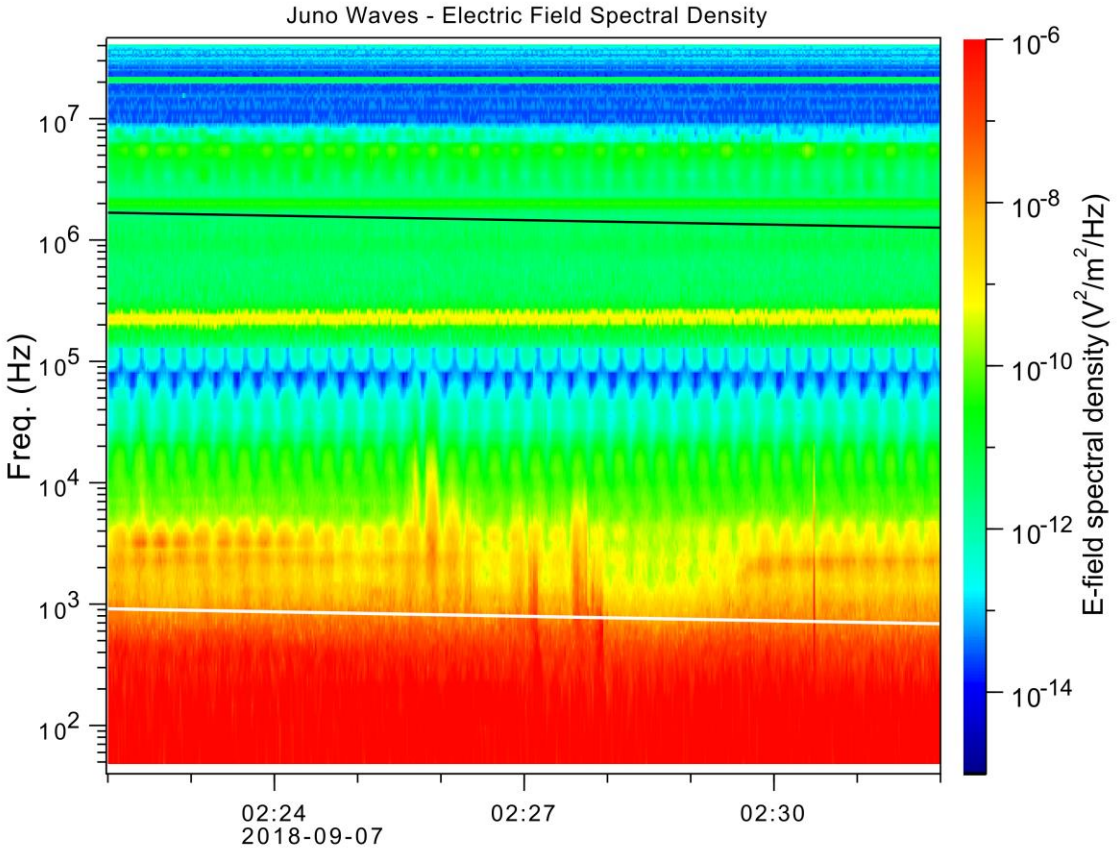

Figure S6. Electric field spectral density from whistler mode wave observations taken by Juno Waves instrument over the Jovian polar regions during PJ15. The black line indicates the range of electron cyclotron frequency, and the white line indicates the range of the proton cyclotron frequency.

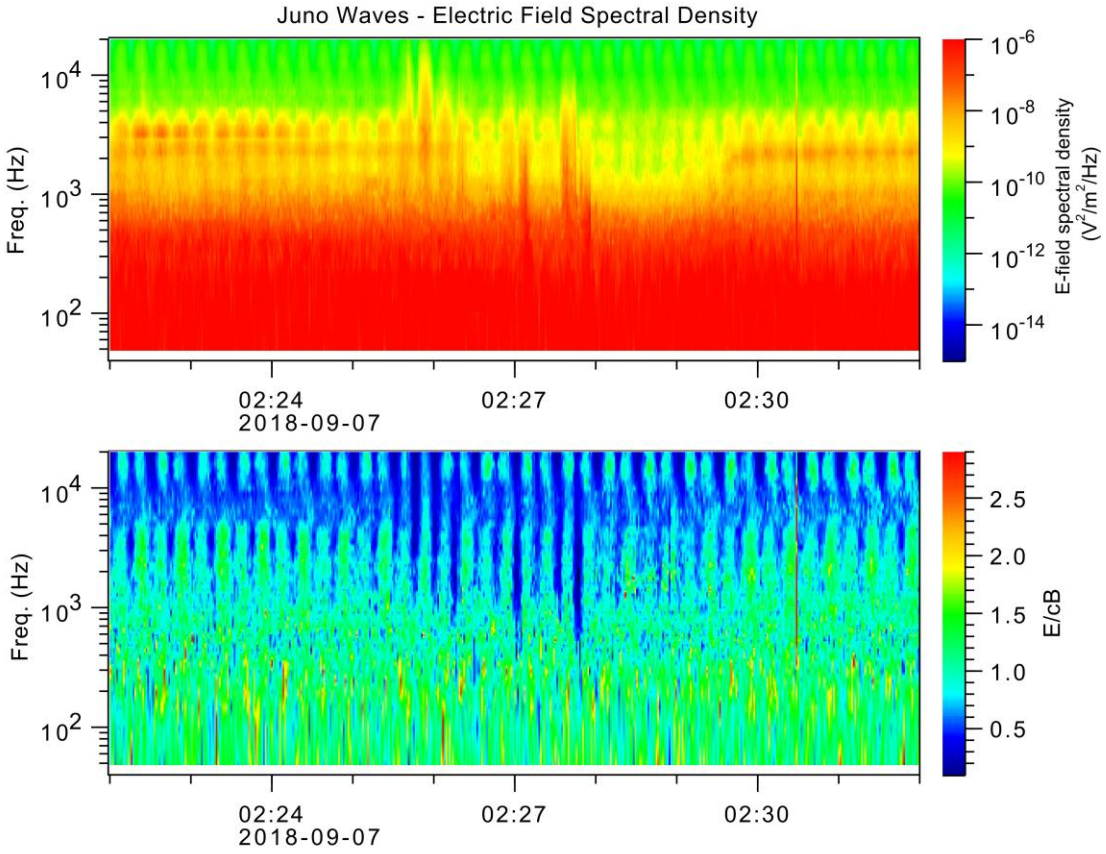

Figure S7. (Top) Electric field spectral density from whistler mode wave observations taken by Juno Waves instrument over the Jovian polar regions during PJ15. (Bottom) Frequency-time spectrogram of the E/cB ratio.

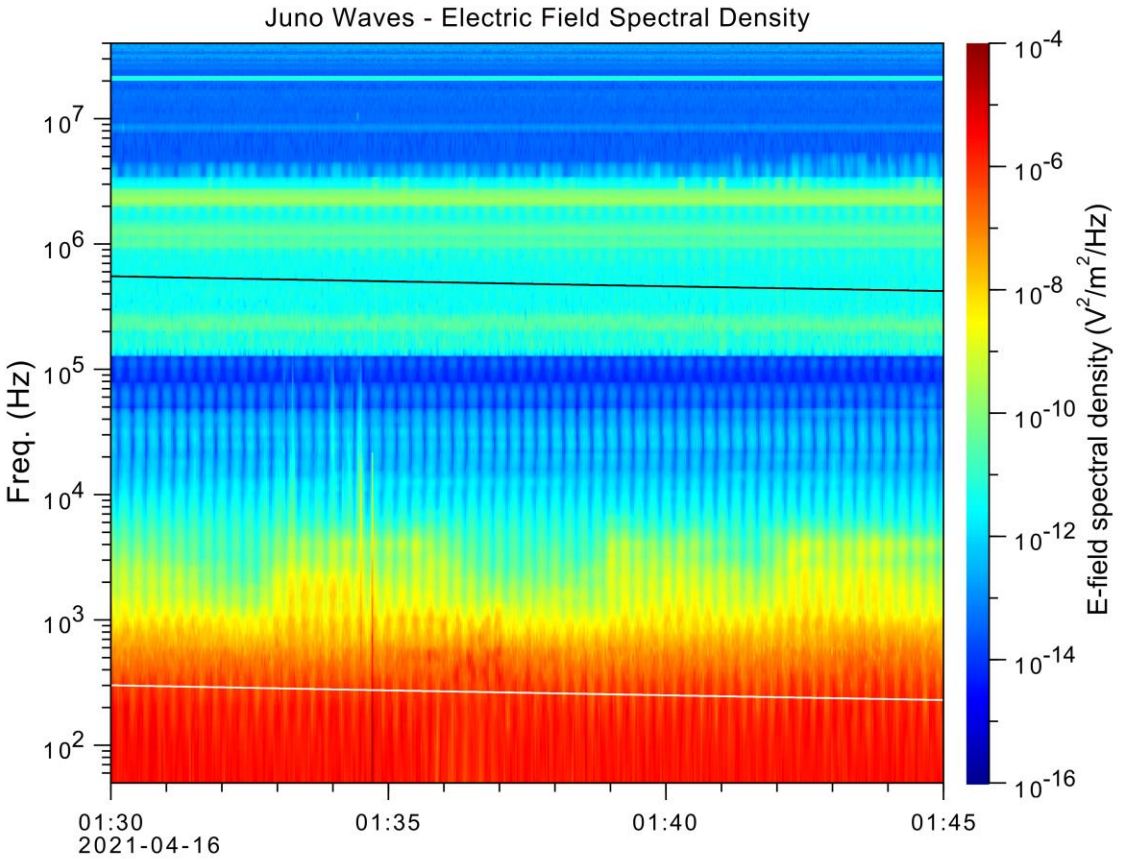

Figure S8. Electric field spectral density from whistler mode wave observations taken by Juno Waves instrument over the Jovian polar regions during PJ33. The black line indicates the range of electron cyclotron frequency, and the white line indicates the range of the proton cyclotron frequency.

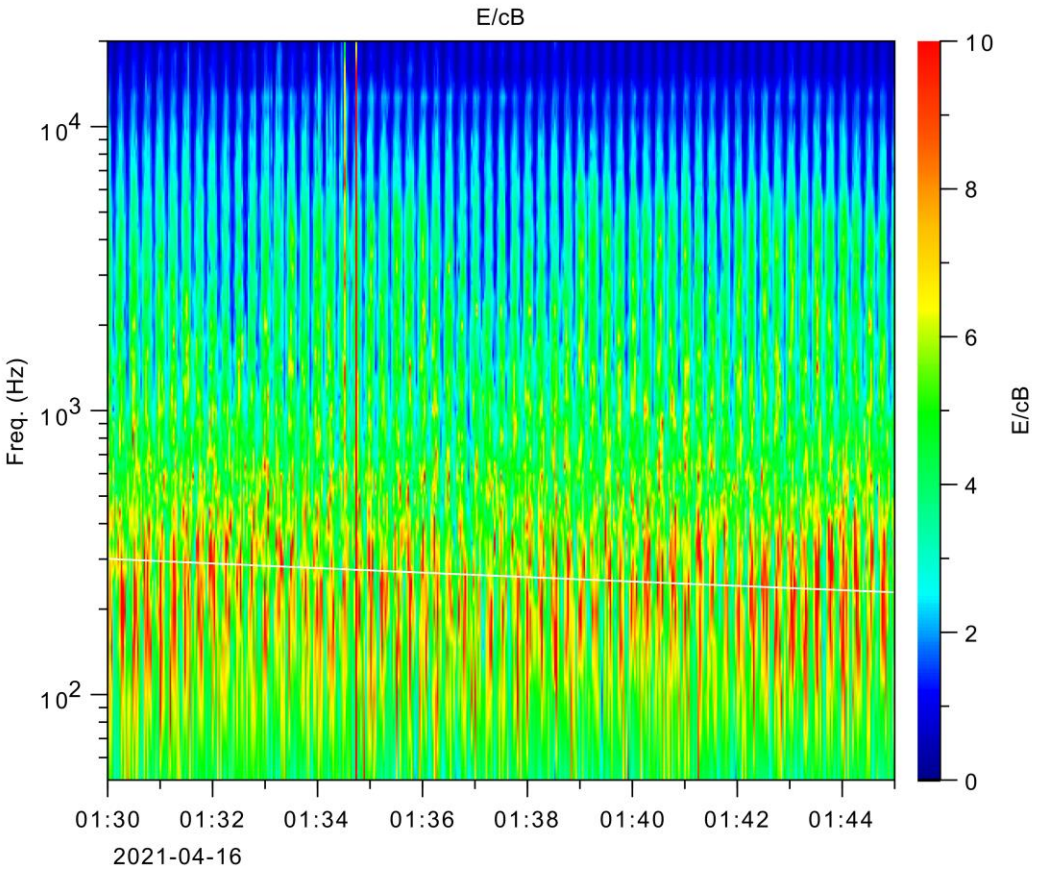

Figure S9. Frequency-time spectrogram of the E/cB ratio during PJ33. The white line indicates the range of the proton cyclotron frequency.